Circadian Capture of Dense-Core Vesicles Rhythmically Boosts Presynaptic Neuropeptide Content in a Clock Neuron

Markus K. Klose[1], Junghun Kim[1], Brigitte F. Schmidt[2], David L. Deitcher[3], and Edwin S. Levitan[1]*

[1] Department of Pharmacology and Chemical Biology, University of Pittsburgh, Pittsburgh, PA 15261, USA

[2] Department of Chemistry, Carnegie Mellon University, Pittsburgh, PA, 15213, USA

[3]Department of Neurobiology and Behavior, Cornell University, Ithaca, NY 14853, USA

*Corresponding author: elevitan@pitt.edu

Key words: secretory granules, axonal transport, vesicle circulation, circadian rhythm, *Drosophila*

20 pages

5 figures

The authors declare no competing interests.

Abstract

Synaptic neuropeptide release by *Drosophila* sLNv clock neurons controls circadian behaviors and sleep. Strikingly, neuropeptide content in sLNv terminals is itself rhythmic with late-night accumulation occurring post-translationally in preparation for midmorning exocytosis of neuropeptide-containing dense-core vesicles (DCVs). Here, live imaging in the brain identifies the mechanism for the daily surge in sLNv presynaptic neuropeptide content. First, consistent with vesicle circulation, sLNv DCVs labeled during synaptic kiss and run exocytosis via a fluorogen-activating protein (FAP) undergo bidirectional transport. Second, anterograde transport to terminals is constant throughout the day. This shows the daily increase in presynaptic neuropeptide content is not produced by a greater supply of DCVs from the soma. Rather, the daily boost in neuropeptide content is accompanied by decreased retrograde axonal DCV transport, which is indicative of increased capture from circulating DCVs. Third, this capture occurs late at night before the daily increase in Ca^{2+} spike activity at nerve terminals and is independent of concurrent IP_3 signaling and axon arbor plasticity. Finally, a *per* gene mutation implicates the circadian clock in rhythmic DCV capture. Thus, clock-dependent capture of circulating DCVs promotes the subsequent daily burst of peptidergic synaptic transmission by sLNv clock neurons.

Introduction

Drosophila sLNv clock neurons release two neuropeptides (PDF and sNPF) that are co-packaged in the same dense-core vesicles (DCVs) (Yu *et al.*, 2025) to regulate circadian behavior (Crespo-Flores and Barber, 2022) and sleep (Shang *et al.*, 2013). Interestingly, PDF content in sLNv neurons is rhythmic based on the function of the circadian clock (Park *et al.*, 2000), which is a feature shared by other neuropeptides in other clock neurons (Hermann-Luibl *et al.*, 2014; Fujiwara *et al.*, 2018; Diaz *et al.*, 2019; Sekiguchi *et al.*, 2024). For both PDF and an exogenously expressed fluorescent protein-tagged neuropeptide, activity-dependent DCV exocytosis decreases presynaptic sLNv terminal neuropeptide content at midmorning (Park *et al.*, 2000; Klose *et al.*, 2021, 2025). Furthermore, rhythmic synaptic release is preceded by a late-night post-translational upregulation of terminal neuropeptide content (Park *et al.*, 2000; Klose *et al.*, 2021) that is advantageous because synaptic neuropeptide release scales with presynaptic neuropeptide content (Bulgari *et al.*, 2014). However, the mechanism for the rhythmic neuropeptide increase in terminals is not known.

Traditionally, it was thought that newly synthesized DCVs are delivered to terminals from the soma for exocytotic release by anterograde axonal transport and eventually delivered back to the soma for degradation by retrograde axonal transport (Alonso and Assenmacher, 1983). In this context, the observed decrease in soma neuropeptide content preceding the increase in terminal neuropeptide content in sLNv terminals (Park *et al.*, 2000; Klose *et al.*, 2021) is intriguing because it is consistent with a surge in anterograde transport producing the daily increase in terminal content (Fig. 1Ai). However, recent studies showed there is late-night DCV exocytosis and

neuropeptide release at the sLNv soma (Klose *et al.*, 2021, 2025), which might fully account for the somatic neuropeptide decrease. In the latter case, another mechanism must explain the daily neuropeptide increase in terminals. Such a mechanism was discovered in the peripheral nervous system where activity increases capture of DCVs as they circulate between distal endings and an axonal region near the soma (Shakiryanova *et al.*, 2006; Wong *et al.*, 2012; Cavolo *et al.*, 2016). Experimentally, induced capture is evident from a drop in retrograde DCV transport that accompanies increased synaptic neuropeptide content (Shakiryanova *et al.*, 2006) (Fig. 1Aii). Thus, two mechanisms for increasing synaptic neuropeptide content are distinguished by their effects on axonal transport: either anterograde vesicle transport is increased or retrograde vesicle transport is decreased by capture of vesicles undergoing bidirectional transport (circulation). In the fly neuromuscular junction, enhanced DCV capture replenishes synaptic neuropeptide content following exogenously stimulated neuropeptide release (Shakiryanova *et al.*, 2006; Cavolo *et al.*, 2016). Thus, along with transport for DCV synaptic exocytosis and degradation, DCV capture during vesicle circulation maintains presynaptic neuropeptide content to respond to the demand produced by synaptic release.

Here, DCV axonal transport is imaged in the adult *Drosophila* brain. Consistent with vesicle circulation, DCV axonal transport in sLNv axons is bidirectional regardless of whether DCVs are labeled upon synthesis in the soma or following kiss and run exocytosis at terminals. Furthermore, rhythmic accumulation of neuropeptide-containing DCVs in sLNv terminals occurs without a change in anterograde axonal transport. Instead, a late-night decrease in retrograde transport reveals an enhancement of

vesicle capture that upregulates neuropeptide content in the sLNv terminals. Because DCV capture occurs before the daily rise in sLNv neuron activity (Klose *et al.*, 2025), follow-up experiments address whether rhythmic presynaptic DCV capture depends on concurrent IP_3 signaling (Klose *et al.*, 2021), axon arbor plasticity (Fernandez et al., 2008; Ispizua et al., 2025) and the circadian clock.

Results and Discussion

DCV axonal transport is consistent with vesicle circulation in a clock neuron

To address the basis of the daily upregulation of neuropeptide content in sLNv terminals, we imaged DCV axonal transport in the adult brain explant from animals with cell specific expression of the DCV marker Dilp2-GFP (Wong *et al.*, 2012), which recapitulates the known PDF content rhythm in sLNv terminals (Klose *et al.*, 2021). Time-lapse imaging in the morning detected DCVs in distal dorsal sLNv axons undergoing both anterograde and retrograde axonal transport (Fig. 1B).

As capture of circulating DCVs could contribute to the daily neuropeptide rhythm in sLNv clock neurons, we sought to test for vesicle circulation in these neurons. Vesicle circulation was established by imaging the body wall innervation of the 2-dimensional filleted larva and conducting FRAP (fluorescence recovery after photobleaching) experiments with a scanning confocal microscope (Shakiryanova et al., 2006; Wong et al., 2012; Cavolo *et al.*, 2016). These experiments are not feasible in the 3-dimensional brain explant because light scattering limits illumination and collection of fluorescence, and photobleaching illumination produces diffusing radicals that induce extensive photodamage. Therefore, we used an alternative approach based on imaging with the

spinning disk confocal microscope, which is very sensitive and produces relatively little photobleaching.

Specifically, experiments took advantage of (a) synaptic neuropeptide release being dominated by kiss and run DCV exocytosis (Wong *et al.*, 2015; Bulgari *et al.*, 2019, 2023; Klose *et al.*, 2021), and (b) the fate of DCVs following exocytosis differing for the traditional model of DCV transport and vesicle circulation: with the former, post-exocytosis DCVs would not undergo anterograde transport because that is reserved for newly synthesized vesicles, while with circulation, bidirectional transport is expected. Therefore, DCVs were selectively labeled by cell specific expression of a neuropeptide tagged with a fluorogen-activating protein (Dilp2-FAP) and application of the membrane impermeant fluorogen MG-TCarb (Bulgari *et al.*, 2019; Klose *et al.*, 2021). With this approach, fluorescence is only produced when the fluorogen diffuses through the fusion pore formed during kiss and run exocytosis to bind the FAP in the DCV lumen. Thus, following the ~1-hour incubation with fluorogen approaching the midmorning peak of synaptic DCV exocytosis and endogenous neuropeptide release at sLNv terminals (i.e., at ZT 2-3) (Klose *et al.*, 2021, 2025), fluorescent DCVs were imaged in distal sLNv axons. In animals co-expressing Dilp2-FAP and Dilp2-GFP, FAP and GFP colocalized in moving axonal puncta (Fig. 2A). Thus, as was found at the NMJ (Bulgari *et al.*, 2019), DCVs were FAP-labeled by kiss and run exocytosis. Furthermore, these post-exocytosis DCVs displayed bidirectional axonal transport (Fig. 2 B,C), which is consistent with delivery of neuropeptides to terminals by vesicle circulation (Fig 1Aii).

Rhythmic capture of circulating DCVs in sLNv terminals

To test for regulated axonal transport of DCVs, we initially measured the number of vesicles being transported per minute (flux) and calculated the ratio of anterograde to retrograde DCV flux (A/R), which is independent of the number of axons sampled. Kymograph analysis (Fig. 3A,B) showed that the flux ratio changed ($P < 0.001$, one-way ANOVA) with a peak at ZT 23 (Fig. 3 A,B). Therefore, there is a net increase in axonal transport of DCVs to sLNv terminals late at night in preparation for the midmorning burst of synaptic neuropeptide release.

Anterograde and retrograde DCV transport fluxes were then examined to determine which component of the flux ratio changed, the numerator (A) or the denominator (R). Analysis of axonal transport showed that anterograde DCV flux (A) was constant at all times tested (Fig. 3C), thus ruling out rhythmic changes in the ratio being driven by changes in anterograde axonal transport from the soma. Rather, retrograde axonal DCV flux (R) cycled ($P < 0.01$, one-way ANOVA) with a minimum late at night at ZT 23 (Fig. 3D). This drop in retrograde flux cannot be explained by exocytosis-induced DCV depletion since the flux drop precedes daily synaptic DCV exocytosis and native synaptic neuropeptide release by several hours (Klose *et al.*, 2021, 2025). Furthermore, the decrease in retrograde flux occurred without altering the velocity of DCVs undergoing retrograde axonal transport (Fig. 3E), thereby excluding a slowing of the retrograde transport motors. The observed reduction in retrograde flux hours before synaptic release with no change in retrograde velocity is indicative of increased synaptic capture of circulating DCVs (Bulgari *et al.*, 2006; Wong *et al.*, 2012; Cavolo *et al.*, 2016). Therefore, increased DCV capture, as opposed to greater DCV

delivery by anterograde transport, produces the daily increase in synaptic neuropeptide content.

DCV capture is independent of rhythmic activity, IP_3 signaling and axon plasticity

The late-night (ZT 23) synaptic capture of DCVs precedes the daily rise in Ca^{2+} spiking, which peaks 4 hours later at midmorning (Klose *et al.*, 2025). However, Ca^{2+} release from endoplasmic reticulum participates in DCV capture at the NMJ (Wong *et al.*, 2009) and there is IP_3-IP3R signaling in sLNv neurons at ZT 23 (Klose *et al.*, 2021). Therefore, we tested for a role of IP_3-IP3R signaling in late-night synaptic DCV capture. Specifically, the flux ratio at ZT 23 was determined after cell specific expression of IP_3 sponge (Uchiyama *et al.*, 2002), which sequesters IP_3, or a dominant negative subunit that disables the IP3R (Sharma and Hasan, 2014). IP_3 sponge did not block capture at ZT 23 (Fig. 4A). Therefore, Ca^{2+} elevation induced by either activity or IP_3 signaling is not required for late-night DCV capture in the presynapse.

We then considered whether the rhythmic DCV capture is linked to daily morphological plasticity in the sLNv axonal arbor (Fernandez *et al.*, 2008). For this purpose, DCV axonal transport was studied in a PDF receptor (PDFR) null mutant (*han*), which prevents daily changes in terminal morphology while preserving rhythmic changes in PDF (Herrero *et al.*, 2020). In PDFR null animals, the daily rhythmic changes in axonal flux ratio persisted (Fig. 4B). Therefore, the daily rhythm in DCV capture occurs independently of PDFR expression and the accompanying axonal plasticity it drives.

Rhythmic DCV capture requires the circadian clock

The PDFR null mutant also abolishes morning anticipation behavior (i.e., the increase in motor activity prior to sunrise) (Hyun *et al.*, 2005). Because rhythmic capture occurs concurrently with this clock-dependent increase in locomotor behavior but persists when morning anticipation is disrupted by the PDFR null mutation, we considered whether capture depends on the circadian clock. If capture is independent of the circadian clock, rhythmic capture would likely be driven through environmental cues, namely daily changes in light levels, and thus would be disrupted after shifting to a constant level of illumination. However, after shifting to constant darkness (DD) capture remained different between CT 23 and CT 3 (Fig. 5, CON). To further test for a role of the circadian clock under DD conditions, we examined the effect of a null mutation in the *period* gene (per^{01}), which is a critical component of the molecular clock. Consistent with the loss of oscillation in synaptic PDF content with this mutant (Park *et al.*, 2000), elevated capture under DD conditions was disrupted in per^{01} animals (Fig. 5, *per*). Therefore, the circadian clock controls rhythmic expansion of the presynaptic neuropeptide pool by vesicle capture.

Conclusions

In *Drosophila* sLNv clock neurons, there is a daily posttranslational surge in synaptic PDF content (Park *et al.*, 2000), which is also evident with an exogenous neuropeptide (Klose *et al.*, 2021). Here, imaging axonal transport in the *Drosophila* brain demonstrated clock-dependent capture of circulating DCVs, rather than increased anterograde axonal transport, rhythmically elevates presynaptic neuropeptide content in sLNv neurons. Because synaptic neuropeptide release is proportional to presynaptic

neuropeptide content (Bulgari *et al.*, 2014), midmorning peptidergic synaptic transmission that controls circadian behavior via PDF is promoted by clock-dependent late-night synaptic capture of circulating DCVs.

Two mechanisms of DCV capture were discovered in the fly NMJ, constitutive capture, which maintains neuropeptide content during quiescence by sequestering DCVs undergoing bidirectional transport, and activity-dependent capture, which replenishes presynaptic neuropeptide stores for minutes following release by tapping into anterograde DCV flux (Shakiryanova et al., 2006; Wong *et al.*, 2012; Cavolo *et al.*, 2016). In contrast, capture in the sLNv clock terminals does not occur in response to the synaptic activity, but rather is driven by the clock (Fig. 5) and is therefore predictive of future activity and synaptic release***.*** Rhythmic DCV capture in sLNv terminals is independent of axonal plasticity (Fig. 4C), thus excluding daily neuropeptide accumulation simply reflects capture to occupy the expanding synaptic arbor. Also, daily DCV capture does not require IP_3 signaling, which is concurrent with, but independent of, increased capture (Fig. 4A,B). Future studies may be able to resolve whether the clock enhances constitutive vesicle capture or activates a distinct mechanism hours in advance of synaptic neuropeptide release.

Clock-dependent vesicle capture likely also upregulates presynaptic sNPF, a neuropeptide that is co-packaged in the same sLNv neuron DCVs as PDF and promotes nighttime sleep (Shang *et al.*, 2013; Yu *et al.*, 2025). Unlike PDF, sNPF gene expression in sLNv neurons is rhythmic (Kula-Eversole *et al.*, 2010), suggesting that both neuropeptide synthesis in the soma and vesicle capture in terminals act synergistically to rhythmically upregulate presynaptic sNPF stores for peptidergic

transmission. It will be of interest to determine how clock neurons in *Drosophila* and mammals utilize clock-regulated vesicle capture and changes in neuropeptide gene expression to control rhythmic behaviors.

Materials and methods

Imaging: Flies were entrained for at least for 72 hours in a 12-hour light: 12-hour dark (LD) schedule before dissection of 4-9 day old males to generate brain explants. Dissections during the dark phase were performed under a red light. Adult flies were immobilized with CO_2 gas and brains were dissected in 0 Ca^{2+} HL3 saline solution (70 mM NaCl, 5 mM KCl, 20 mM $MgCl_2$*$6H_2O$, 115 mM Sucrose, 5 mM Trehalose, 5 mM Hepes, and 10 mM $NaHCO_3$, pH 7.3) and brain explants were then put into polylysine-coated plastic dishes containing HL3 with 2 mM Ca^{2+} (Klose et al., 2016). sLNv somas are located on the ventral side of the Drosophila brain and send axons to the dorsal protocerebrum, thus brain explants were viewed from the dorsal surface of the brain so that DCVs in the distal axon could be imaged with the dipping water immersion objective of an upright spinning disk confocal microscope. Imaging was done on setups with an upright Olympus microscope equipped with a 60× 1.1 NA dipping water immersion objective, a Yokogawa spinning disk confocal head, a Teledyne Photometrics sCMOS camera, and lasers for illumination (488 nm for GFP and 640 nm for FAP). In some experiments, a recombinant with UAS-Dilp2-GFP and UAS-Dilp2-FAP was used so that GFP could be viewed for focusing before application of the membrane impermeant fluorogen MG-Tcarb (Klose *et al.*, 2021). For DCV axonal transport, two axonal regions in the dorsal protocerebrum were imaged in each

hemisphere of the brain. Time-lapse experiments entailed acquiring 180 images with 35-150 ms exposure times at 3 Hz. From these movies, regions where dorsally projecting axons defasciculated from bundles were used for generating kymographs with the Kymograph plugin of ImageJ. Quantification was done in Imagej or Fiji. Statistical analysis (i.e., tests and calculation of standard error of the mean (SEM) for error bars) was performed with Graphpad Prism software.

Fly lines: All flies used the PDF-GAL4 promoter on the third chromosome (provided by Paul Taghert, Washington University in St. Louis). UAS-Dilp2-GFP and UAS-Dilp2-FAP were reported previously (Wong *et al.*, 2012; Bulgari *et al.*, 2019). w^{1118} flies were from Zachary Freyberg (University of Pittsburgh). Fly lines from the Bloomington *Drosophila* stock center included *Bl#* 33068 (*han*) and *Bl#* 80917 (per^{01}). The IP_3 sponge line was provided by C. Andrew Frank (University of Iowa) and the IP3R dominant negative line was provided by Gaiti Hasan (Tata Institute of Fundamental Research).

Acknowledgments

We thank Drs. C.A. Frank and G. Hasan for kindly providing IP_3 signaling-related flies. Stocks obtained from the Bloomington Drosophila Stock Center (NIH P40OD018537) were used in this study. Research reported in this publication was supported by the National Institute Of Neurological Disorders And Stroke of the National Institutes of Health under Award Number R01NS032385 to ESL. The content is solely the responsibility of the authors and does not necessarily represent the official views of the National Institutes of Health.

References

Alonso G, Assenmacher I. Retrograde axoplasmic transport of neurosecretory material. An immunocytochemical and electron-microscopic study of transected axons in normal and colchicine-treated rats. Cell Tissue Res. 1983;233(1):183-96.

Bulgari D, Cavolo SL, Schmidt BF, Buchan K, Bruchez MP, Deitcher DL, Levitan ES. Ca2+ and cAMP open differentially dilating synaptic fusion pores. J Cell Sci. 2023 Jul 1;136(13):jcs261026. doi: 10.1242/jcs.261026. Epub 2023 Jul 4. PMID: 37303204; PMCID: PMC10357034.

Bulgari D, Deitcher DL, Schmidt BF, Carpenter MA, Szent-Gyorgyi C, Bruchez MP, Levitan ES. Activity-evoked and spontaneous opening of synaptic fusion pores. Proc Natl Acad Sci U S A. 2019 Aug 20;116(34):17039-17044. doi: 10.1073/pnas.1905322116. Epub 2019 Aug 5. PMID: 31383765; PMCID: PMC6708360.

Bulgari D, Zhou C, Hewes RS, Deitcher DL, Levitan ES. Vesicle capture, not delivery, scales up neuropeptide storage in neuroendocrine terminals. Proc Natl Acad Sci U S A. 2014;111(9):3597-601.

Cavolo SL, Bulgari D, Deitcher DL, Levitan ES. Activity induces Fmr1-sensitive synaptic capture of anterograde circulating neuropeptide vesicles. J Neurosci. 2016;36(46):11781-11787.

Crespo-Flores SL, Barber AF. The Drosophila circadian clock circuit is a nonhierarchical network of peptidergic oscillators. Curr Opin Insect Sci. 2022; 52:100944.

Díaz MM, Schlichting M, Abruzzi KC, Long X, Rosbash M. Allatostatin-C/AstC-R2 Is a Novel Pathway to Modulate the Circadian Activity Pattern in Drosophila. Curr Biol. 2019 Jan 7;29(1):13-22.e3. doi: 10.1016/j.cub.2018.11.005. Epub 2018 Dec 13. PMID: 30554904; PMCID: PMC6325008.

Fernández MP, Berni J, Ceriani MF. Circadian remodeling of neuronal circuits involved in rhythmic behavior. PLoS Biol. 2008 Mar 25;6(3):e69. doi: 10.1371/journal.pbio.0060069. PMID: 18366255; PMCID: PMC2270325.

Fujiwara Y, Hermann-Luibl C, Katsura M, Sekiguchi M, Ida T, Helfrich-Förster C, Yoshii T. The CCHamide1 Neuropeptide Expressed in the Anterior Dorsal Neuron 1 Conveys a Circadian Signal to the Ventral Lateral Neurons in Drosophila melanogaster. Front Physiol. 2018 Sep 10;9:1276. doi: 10.3389/fphys.2018.01276. PMID: 30246807; PMCID: PMC6139358.

Hermann-Luibl C, Yoshii T, Senthilan PR, Dircksen H, Helfrich-Förster C. The ion transport peptide is a new functional clock neuropeptide in the fruit fly Drosophila melanogaster. J Neurosci. 2014 Jul 16;34(29):9522-36. doi:

10.1523/JNEUROSCI.0111-14.2014. PMID: 25031396; PMCID: PMC6608324.

Herrero A, Yoshii T, Ispizua JI, Colque C, Veenstra JA, Muraro NI, Ceriani MF. Coupling Neuropeptide Levels to Structural Plasticity in Drosophila Clock Neurons. Curr Biol. 2020;30(16):3154-3166.e4.

Hyun S, et al. Drosophila GPCR Han is a receptor for the circadian clock neuropeptide PDF. Neuron. 2005; 48(2):267-278.

Ispizua JI, Rodríguez-Caron M, Tassara FJ, Kim KY, Insussarry Perkins C, Barzi M, Carpio-Romero C, Vasquez MF, Hansen CN, Gargiulo J, Rosato E, de la Iglesia H, Ellisman MH, Ceriani MF. Daily ultrastructural remodeling of clock neurons. bioRxiv [Preprint]. 2025 Feb 13:2024.11.06.622332. doi: 10.1101/2024.11.06.622332. PMID: 39990321; PMCID: PMC11844358.

Klose MK, Bruchez MP, Deitcher DL, Levitan ES. Temporally and spatially partitioned neuropeptide release from individual clock neurons. Proc Natl Acad Sci U S A. 2021;118(17):e2101818118.

Klose MK, Kim J, Gregg SN, Schmidt BF, Xia X, Li Y, Levitan ES. Desynchronized Somas and Terminals in a Morning Clock Neuron: Presynaptic Ca 2+ Spiking and Native Neuropeptide Release Peak As Somatic Ca 2+ Declines. bioRxiv [Preprint]. 2025 Aug 12:2023.12.01.569590. doi: 10.1101/2023.12.01.569590. PMID: 38106047;

PMCID: PMC10723267.

Kula-Eversole E, Nagoshi E, Shang Y, Rodriguez J, Allada R, Rosbash M. Surprising gene expression patterns within and between PDF-containing circadian neurons in Drosophila. Proc Natl Acad Sci U S A. 2010 Jul 27;107(30):13497-502. doi: 10.1073/pnas.1002081107. Epub 2010 Jul 12. PMID: 20624977; PMCID: PMC2922133.

Moughamian AJ, Holzbaur EL. Synaptic vesicle distribution by conveyor belt. Cell. 2012 Mar 2;148(5):849-51. doi: 10.1016/j.cell.2012.02.007. PMID: 22385955.

Park JH, Helfrich-Förster C, Lee G, Liu L, Rosbash M, Hall JC. Differential regulation of circadian pacemaker output by separate clock genes in Drosophila. Proc Natl Acad Sci U S A. 2000;97(7):3608-13.

Sekiguchi M, Katoh S, Yokosako T, Saito A, Sakai M, Fukuda A, Itoh TQ, Yoshii T. The Trissin/TrissinR signaling pathway in the circadian network regulates evening activity in Drosophila melanogaster under constant dark conditions. Biochem Biophys Res Commun. 2024 Apr 16;704:149705. doi: 10.1016/j.bbrc.2024.149705. Epub 2024 Feb 22. PMID: 38430699.

Shakiryanova D, Tully A, Levitan ES. Activity-dependent synaptic capture of transiting peptidergic vesicles. Nat Neurosci. 2006 Jul;9(7):896-900. doi: 10.1038/nn1719. Epub

2006 Jun 11. PMID: 16767091.

Shang Y, Donelson NC, Vecsey CG, Guo F, Rosbash M, Griffith LC. Short neuropeptide F is a sleep-promoting inhibitory modulator. Neuron. 2013 Oct 2;80(1):171-83. doi: 10.1016/j.neuron.2013.07.029. Epub 2013 Oct 2. PMID: 24094110; PMCID: PMC3792499.

Sharma A, Hasan G. Modulation of flight and feeding behaviours requires presynaptic IP3Rs in dopaminergic neurons. Elife. 2020 Nov 6;9:e62297. doi: 10.7554/eLife.62297. PMID: 33155978; PMCID: PMC7647402.

Wong MY, Zhou C, Shakiryanova D, Lloyd TE, Deitcher DL, Levitan ES. Neuropeptide delivery to synapses by long-range vesicle circulation and sporadic capture. Cell. 2012;148(5):1029-38.

Yu J, Zhang Y, Clements K, Chen N, Griffith LC. Genetically-encoded markers for confocal visualization of single dense core vesicles. Commun Biol. 2025;8(1):383.

Figure Legends

Figure 1. How does DCV transport produce daily increase in sLNv nerve terminal neuropeptide content?

A. Schematics present two hypotheses for how DCV transport dynamics could increase neuropeptide content at sLNv nerve terminals late at night and prior to release. Ai. Timed increase in anterograde transport of DCVs to nerve terminals late at night. Aii. Timed increase in capture of circulating DCVs late at night resulting in reduced retrograde transport. Bi. sLNv projections containing DCVs labeled with Dilp2-GFP were imaged at 3 Hz. White box reveals region of interest (ROI) for analysis. Bii. DCVs at t = 0, 0.33, 0.66, and 1.0 seconds (red arrow indicates anterograde (AR) transport and blue arrow indicates retrograde (RE) transport, scale bar = 1 μm). Biii. Kymograph of ROI (red arrow anterograde, blue arrow retrograde transport).

Figure 2. Post-exocytosis DCVs display bidirectional axonal transport.

A. Co-localization of GFP and FAP signal in moving puncta through sLNv nerve terminals of UAS-Dilp2-GFP, UAS-Dilp2-FAP; PDF-Gal4 flies (slope down, left to right). AN= anterograde transport (red arrow). B. FAP-labeled puncta in sLNv nerve terminals reveal both anterograde and retrograde mobility. RE= Retrograde transport (blue arrow). C. Kymographs reveal both anterograde (slope down, left to right) and retrograde (slope down, right to left) DCV axonal transport in sLNv projections.

Figure 3. Daily Rhythm in DCV capture.

A. Kymographs reveal both anterograde (slope down, left to right) and retrograde (slope down, right to left) DCV axonal transport in sLNv projections of PDF>Dilp2-GFP flies at ZT 3 and ZT 23. B. Flux ratios (anterograde/retrograde) at different times of the day. n values (number of hemibrains) for ZT 1, 3, 5, 7, 11, 13, 17, 19, 21, 23 are 4, 10, 6, 6, 8, 6 ,8, 8, 4, 12, respectively. One-way ANOVA revealed significant difference ($P < 0.001$). Post-test analysis by Dunnett's multiple-comparison test is presented: ****$P < 0.0001$, ***$P < 0.001$, *$P < 0.05$. C. Anterograde flux and D. Retrograde flux (vesicles/min) in PDF>Dilp2-GFP brains. The n values for ZT 2-4, 8-10, 14-16, and 23 are 11,12,10, and 9, respectively. $P < 0.01$, one-way ANOVA. **$P < 0.01$, *$P < 0.05$, Tukey's multiple-comparison post-test.E. Retrograde velocity of DCVs at ZT 3 and 23 in PDF>Dilp2-GFP brains (left, average per brain; ZT 3 n = 4, ZT 23 n = 4; right, individual vesicle measurements: ZT 3 n = 49, ZT 23 n = 51).

Figure 4. Rhythmic capture does not require concurrent IP_3 signaling or PDFR-induced axonal plasticity.

A. Ratios of anterograde to retrograde DCV flux (A/R) at ZT 3 and ZT 23 in *w*; UAS-Dilp2-GFP; PDF-GAL4 controls (CON) and IP_3 sponge; UAS-Dilp2-GFP; PDF-GAL4 UAS-IP_3 sponge sLNv axons. n $\geq$ 13 for CON; n > 9 for IP_3 sponge. For both CON and *han*, ****$P < 0.0001$, unpaired t-test. B. Ratios of anterograde to retrograde DCV flux (A/R) at ZT 3 and ZT 23 in *w*; UAS-Dilp2-GFP; PDF-GAL4 controls (CON) and *han*; UAS-Dilp2-GFP; PDF-GAL4 PDFR null (*han*) sLNv axons. n $\geq$ 13 for CON; n > 20 for *han*. For both CON and *han*, ****$P < 0.0001$, unpaired t-test.

Figure 5. Rhythmic DCV capture depends of on *per*.

Ratios of anterograde to retrograde DCV flux (A/R) 2 days after transition to constant darkness at CT3 and CT23 in *w*; UAS-Dilp2-GFP; PDF-GAL4 controls (CON) and $y^1 per^{01} w^*$; *UAS-Dilp2-GFP; PDF-GAL4* (*per*) sLNv axons. n = 9 for CON; n = 6 for CT3 and n = 7 for CT23 in *per* animals. **P < 0.01, unpaired t-test.

A

i

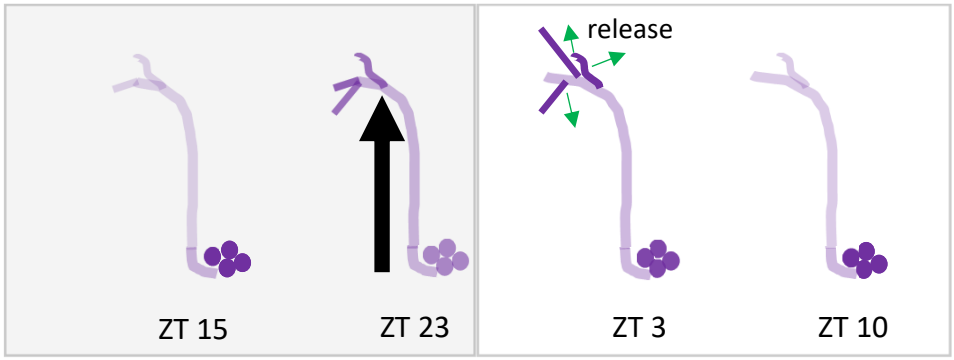

Timed Increase
in TRANSPORT

ii

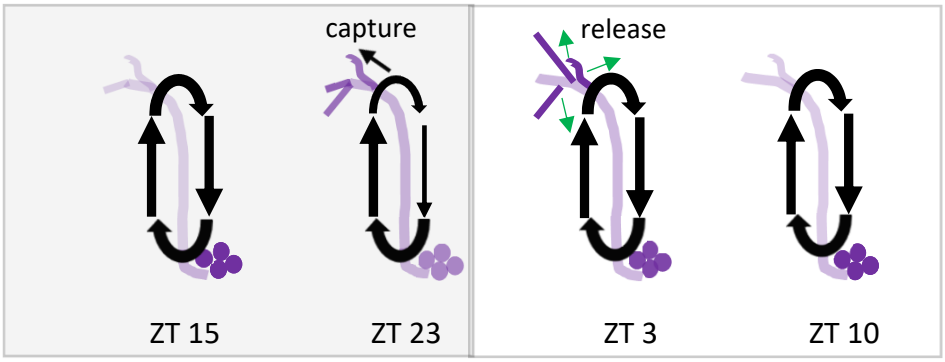

Timed increase
in CAPTURE

Bi

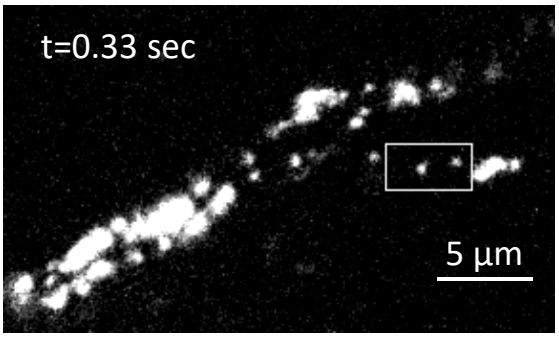

Bii

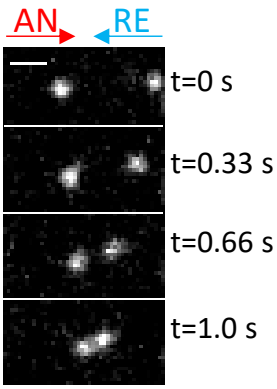

Biii

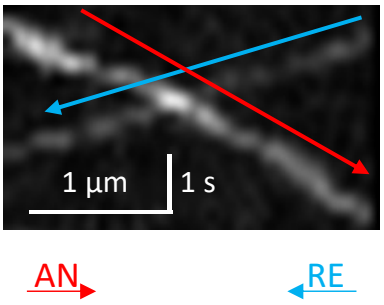

Figure 1

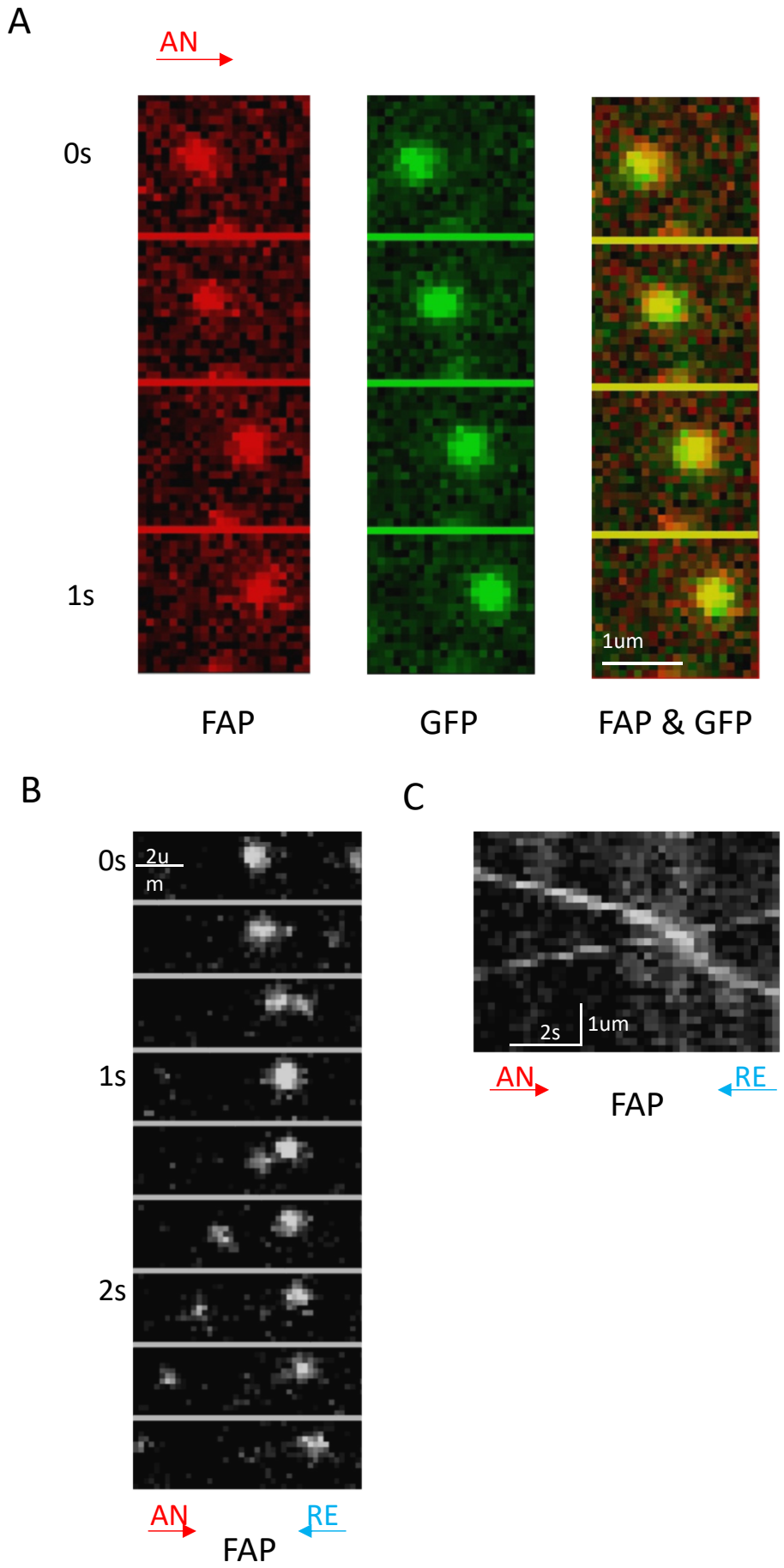
A
AN
0s
1s
1um
FAP
GFP
FAP & GFP
B
0s
2um
1s
2s
AN
RE
FAP
C
2s
1um
AN
RE
FAP

Figure 2

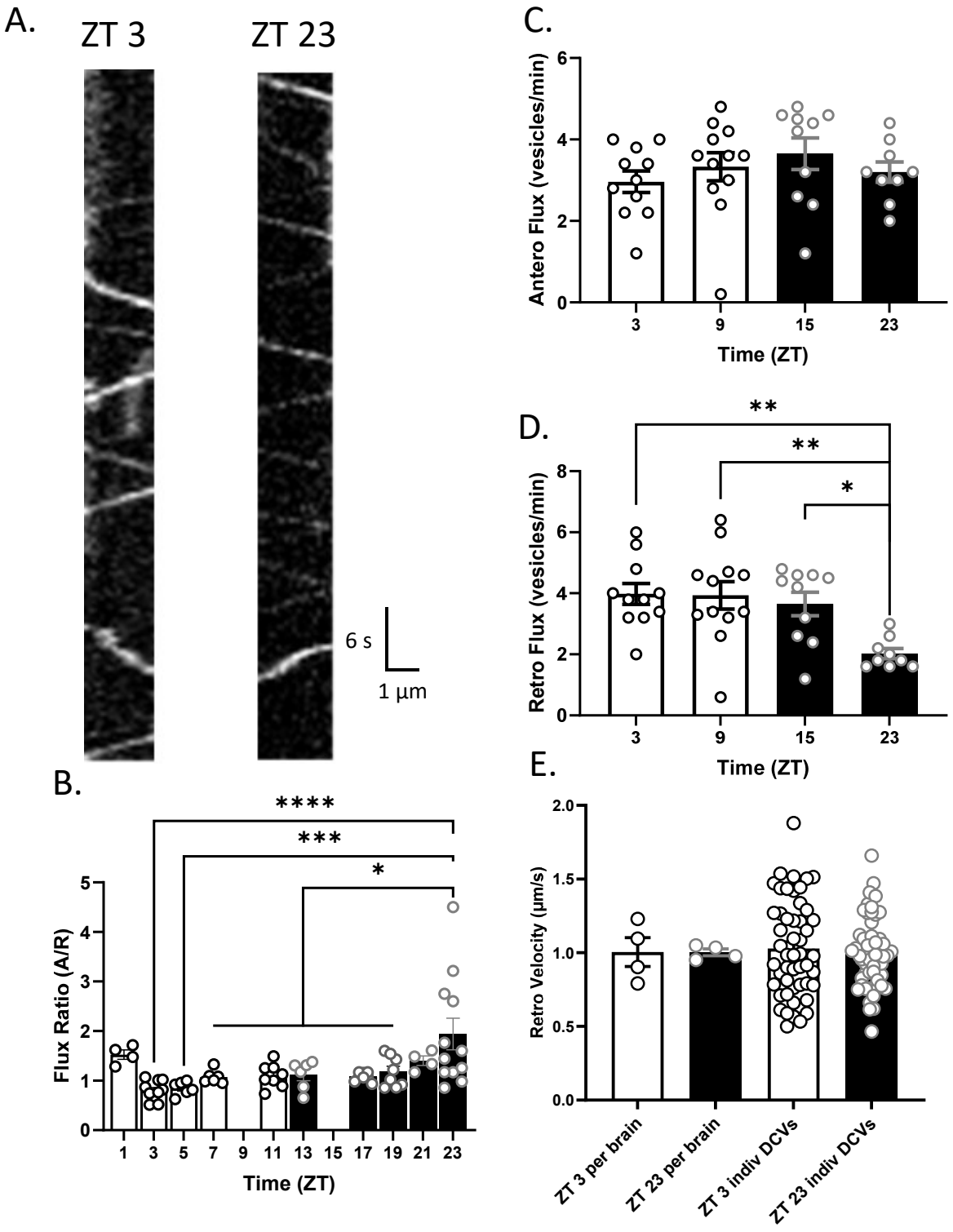
A.
ZT 3
ZT 23
6 s
1 µm
B.
****
***
*
Flux Ratio (A/R)
Time (ZT)
C.
Antero Flux (vesicles/min)
Time (ZT)
D.
**
**
*
Retro Flux (vesicles/min)
Time (ZT)
E.
Retro Velocity (µm/s)
ZT 3 per brain
ZT 23 per brain
ZT 3 indiv DCVs
ZT 23 indiv DCVs

Figure 3

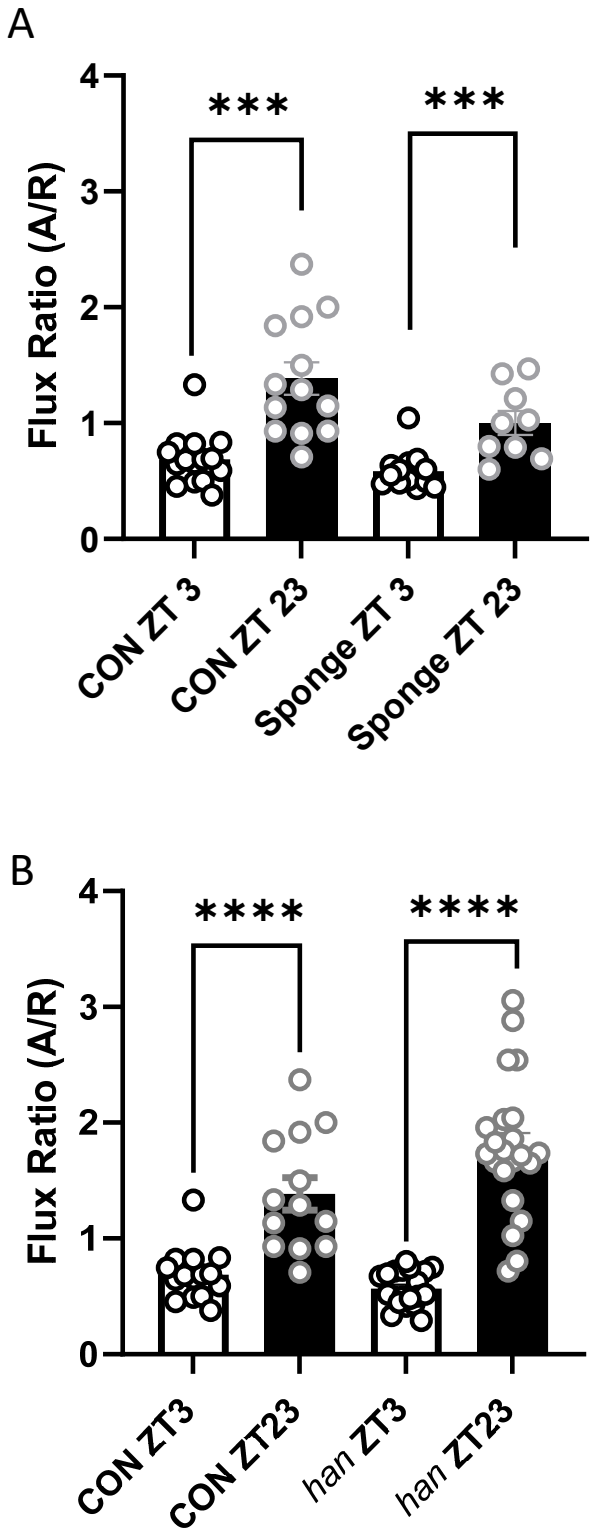
A
Flux Ratio (A/R)
0
1
2
3
4
***
***
CON ZT 3
CON ZT 23
Sponge ZT 3
Sponge ZT 23
B
Flux Ratio (A/R)
0
1
2
3
4
****
****
CON ZT3
CON ZT23
han ZT3
han ZT23

Figure 4

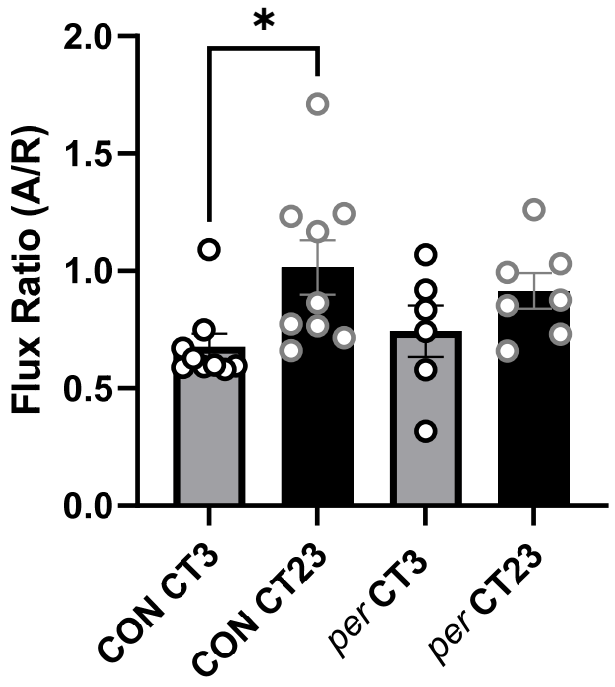

Figure 5